ORIGINAL ARTICLE   **Open Access**

Outside-in signaling by femoral cuff injury induces a distinct vascular lesion in adipose triglyceride lipase knockout mice

Hirotsugu Noguchi[1,2]*, Sohsuke Yamada[1,3]*, Ken-ichi Hirano[4],
Satoshi Yamaguchi[4], Akira Suzuki[4], Xin Guo[3], Nobuhiro Zaima[5,6], Ming Li[4], Kunihisa
Kobayashi[7], Yoshihiko Ikeda[8], Toshiyuki Nakayama[1] and Yasuyuki Sasaguri[1]

[1]Department of Pathology, School of Medicine, University of Occupational and Environmental Health, [2]Department of Pathology,
Field of Oncology, Graduate School of Medical and Dental Sciences, Kagoshima University, Kagoshima, [3]Department of Pathology
and Laboratory Medicine, Kanazawa Medical University, Kanazawa, [4]Laboratory of Cardiovascular Disease, Novel, Non-invasive,
and Nutritional Therapeutics (CNT) and Triglyceride Research Center (TGRC), Department of Triglyceride Science, Graduate School
of Medicine, Osaka University, Osaka, [5]Department of Applied Biological Chemistry, Graduate School of Agriculture, Kindai
University, [6]Agricultural Technology and Innovation Research Institute, Kindai University, Kinday, [7]Department of Endocrinology and
Diabetes Mellitus, Fukuoka University Chikushi Hospital, Fukuoka and [8]Department of Pathology, National Cerebral and
Cardiovascular Center, Osaka, Japan

*these authors equally contributed to this work

Summary. Genetic deficiency of adipose triglyceride lipase (ATGL), a rate-limiting enzyme for intracellular triglyceride (TG) hydrolysis, causes TG-deposit cardiomyovasculopathy (TGCV), a recently identified rare cardiovascular disorder (ORPHA code: 565612) in humans. One of the major characteristics of TGCV is a novel type of diffuse and concentric coronary atherosclerosis with ATGL-deficient smooth muscle cells (SMCs). Patients with TGCV have intractable coronary artery disease. Therefore, it is crucial to investigate the mechanisms underlying vascular lesions in ATGL deficiency using animal models. Cuff injury is an experimental procedure to induce vascular remodeling with neointimal formation with SMCs after placing a cuff around the adventitial side of the artery without direct influence on endothelium. We report the effect of cuff injury on femoral arteries of *ATGL*-knockout (*ATGL*^{−/−}) mice. Cuff-induced concentric neointimal formation with migrating SMCs was exacerbated in *ATGL*^{−/−} mice, mimicking atherosclerotic lesions in patients with TGCV. In the media, cell death of SMCs and loss of elastic fibers increased.

Perivascular infiltrating cells expressing tumor necrosis factor-α (TNF-α) were more prominent in *ATGL*^{−/−} mice than in wild-type (WT) mice. In Boyden chamber experiments, a greater number of *ATGL*^{−/−} SMCs migrated in response to TNF-α compared to WT SMCs. These data, for the first time, demonstrated that outside-in signaling by cuff-induced neointimal formation where paracrine stimuli from adventitial infiltrating cells may lead to neointimal formation and mediolysis in ATGL-deficient conditions. Cuff injury might be a valuable model for understanding the mechanisms underlying the development of atherosclerotic lesions in patients with TGCV

Key words: Adipose triglyceride lipase, Cuff injury, Outside-in signaling, Smooth muscle cell, Triglyceride deposit cardiomyovasculopathy

Introduction

Adipose triglyceride lipase (ATGL) is an essential molecule for intracellular TG hydrolysis (Zimmermann et al., 2004; Haemmerle et al., 2006; Zechner et al., 2009). ATGL is expressed in adipocytes, cardiomyocytes, and vascular smooth muscle cells (SMCs), where ATGL catalyzes triglyceride (TG) and releases long chain fatty acid (LCFA) for mitochondrial β-oxidation (Zimmermann et al., 2004; Haemmerle et al. 2006). We were the first to report that genetic deficiency

of ATGL causes TG-deposit cardiomyovasculopathy (TGCV) in humans (Hirano et al., 2008, 2014; Hirano, 2009). TGCV is now recognized as a rare cardiovascular disorder in which defective intracellular lipolysis leads to severe coronary artery disease and heart failure (ORPHA code: 565612) (Hirano et al., 2019; Li et al., 2019; Nakajima., 2021). One of the major pathological characteristics of TGCV is a unique atherosclerosis with TG deposits in smooth muscle cells SMCs (Ikeda et al., 2014a,b; Hirano et al., 2019; Li et al., 2019), exhibiting diffuse and concentric stenosis, which is in contrast to cholesterol-induced atherosclerosis with focal and eccentric stenosis and cholesterol-laden macrophages (Ross, 1999). Major adverse cardiovascular events, including sudden death, are frequent in patients with TGCV (Hirano et al., 2019; Kozawa et al., 2019; Li et al., 2019; Nakano et al., 2020; Onishi et al., 2021), because cholesterol-lowering therapy is not effective for this condition. Thus, it is crucial to investigate the mechanisms underlying vascular lesion formation in TGCV, using animal models.

There are several classic and modern experimental procedures to induce vascular remodeling and atherosclerosis, such as ligation, endothelial denudation, and dietary interventions, in addition to genetic manipulations (Ross and Glomset, 1973; Daugherty et al., 2017). We induced cuff injury in femoral arteries in *ATGL*-knockout ($ATGL^{-/-}$) mice with severe cardiomyocyte steatosis and premature death (Haemmerle et al., 2006). We chose this experimental setting for the following reasons: 1) cuff injury induces neointimal formation with SMCs (Booth et al., 1989; Kockx et al., 1992; Moroi et al., 1998; Sasaguri et al., 2005; Yamada et al., 2008, 2016), which are the major cellular components of atherosclerotic lesions in TGCV, as described above; 2) we previously reported that SMCs from $ATGL^{-/-}$ mouse aorta exhibit distinct phenotypes with TG deposition in culture (Lin et al., 2013); 3) cuff-induced vascular changes can occur within a couple of weeks, which would enable us to complete the experiments before the $ATGL^{-/-}$ mice died of severe heart failure and mitochondrial dysfunction by the age of 13–15 weeks (Haemmerle et al., 2006); 4) bone marrow transplantation (BMT), which is a powerful procedure, as demonstrated by many research groups including ours (Fazio and Linton, 1996; Sasaguri et al., 2005; Lammers et al., 2011; Guo et al., 2012), was not used in this experiment. This is because BMT focuses on the roles of hematopoietic progenitor cells, including monocytes and macrophages, which do not play central roles in TG-deposit atherosclerosis observed in patients with TGCV, as mentioned above (Lammers et al., 2011; Lin et al., 2013; Ikeda et al., 2014a,b; Hirano et al., 2019).

We analyzed the intimal, medial, and adventitial changes in cuff-injured arteries, performed *in vitro* in Boyden chamber experiments with cultured $ATGL^{-/-}$ SMCs with TG deposition, and discuss the implications from the obtained experimental data.

Materials and methods

Animals and cuff-injured mouse model

Eight-week-old, male, $ATGL^{-/-}$ and C57BL/6J wild-type (WT) mice were used in the experiments (Haemmerle et al., 2006). The average body weight was 26.5±0.5 g for $ATGL^{-/-}$ mice, and 25.7±0.3 g for WT mice. These mice were maintained under standard laboratory conditions (temperature 24±1°C, humidity 55±5%). Drinking water and food were available ad libitum and the mice were maintained on a 12 h light/dark cycle. To produce the cuff model, the right femoral artery was cleared from the perivascular connective tissue through a right inguinal incision and loosely sheathed with a non-constrictive polyethylene cuff (inner/outer diameter: 0.38/1.09 mm, length: 2 mm; PE-20 tubing; Becton Dickinson Labware; Franklin Lakes, NJ, USA) (Moroi et al., 1998; Sasaguri et al., 2005; Yamada et al., 2008, 2016). The procedure was performed under anesthesia with 5.0% v/v sevoflurane (Mylan; Canonsburg, PA, USA). The cuff was double-tied with sterile surgical 7-0 silk sutures (Alfresa Pharma Corp.; Tokyo, Japan). The cuff was larger than the vessel and blood flow was not obstructed. The left femoral artery was also isolated from the surrounding tissue, but a cuff was not placed, and this artery served as the sham-operated control. The control young male WT and $ATGL^{-/-}$ mice, weighing 23-26 g, did not undergo any surgical procedure.

All experimental protocols were approved by the Ethics Committees of Animal Care and Experimentation, University of Occupational and Environmental Health, Japan. The experiments were performed according to the Institutional Guidelines for Animal Experiments and the Law (No. 105) and Notification (No. 6) of the Japanese government. The investigation complies with the ARRIVE guidelines and was carried out in accordance with the Guide for the Care and Use of Laboratory Animals published by the US National Institutes of Health (NIH Publication No. 85-23, revised 1996).

Histopathology

The animals were killed 10 days after surgery, in accordance with the approved guidelines. Both the right and left femoral arteries were excised and bisected from one edge to the other edge of the cuffed portion and the corresponding segment of the contralateral control artery, to obtain an approximately 2 mm specimen from each artery (Sasaguri et al., 2005; Yamada et al., 2016). The relevant portions of the femoral arteries were fixed in 10% neutral buffered formalin for 24 h and embedded in paraffin. Serial cross-sections (4 μm thickness, at 80 μm thickness intervals, 300-500 specimens per mouse) were obtained for hematoxylin and eosin, elastica van Gieson (EVG), Masson's trichrome, and Alcian blue staining or for immunohistochemistry (IHC) (Moroi et al., 1998; Sasaguri et al., 2005; Yamada et al., 2008, 2016). The analyses were performed in the cuff-injured right femoral arteries in all experiments. The proportions of the

elastolytic length to the internal and external elastic lamina, the thickened intimal and medial areas were calculated as described previously (Sasaguri et al., 2005; Yamada et al., 2008, 2011, 2016). Additionally, we calculated the stenotic lumen area, the adventitial area, and total vessel area.

IHC and immunofluorescence (IF) staining studies

The following primary antibodies were used in IHC and IF staining: rat anti-mouse Mac-2 monoclonal antibody (1:500; Cedarlane Laboratories Ltd.; Burlington, Canada) and monoclonal mouse anti-human smooth muscle actin antibody (α-SMA; 1:150; DAKO Cytomation Co.; Tokyo, Japan) were used to detect macrophages and fibroblasts, and SMCs, respectively. For the latter, we used HistoMouse™–*Plus* Kits (Invitrogen Corporation; Camarillo, CA, USA) to block the endogenous mouse IgG (Sasaguri et al., 2005; Yamada et al., 2008, 2011, 2013; Guo et al., 2012; Tasaki et al., 2013). Rat anti-mouse Ly-6G (Gr-1; 1:500; Southern Biotech, Birmingham, AL, USA) antibodies were used to evaluate neutrophil infiltration in the inflamed adventitial lesions (Noguchi et al., 2014). Additionally, monoclonal mouse tumor necrosis factor (TNF)-α (1:50; Abcam; Burlingame, CA, USA) and rat Mac-2 (1:500; Cedarlane Laboratories Ltd.) antibodies were used to detect pro-inflammatory adventitial infiltrating cells in cuffed arteries by double-IF. These slides were developed with Alexa Fluor (*red*) conjugated goat anti-mouse IgG and Alexa Fluor (*green*) conjugated goat anti-rat IgG and IgM antibodies (Invitrogen Corp.), and observed using confocal laser scanning microscopy (LSM5 Pascal Exciter; Carl Zeiss; Oberkochen, Germany; original magnification: 400×) (Sasaguri et al., 2005; Guo et al., 2012; Tasaki et al., 2013; Yamada et al., 2013; Noguchi et al., 2014).

To analyze the proliferative and cell death activity of vascular cells in the neointimal or medial lesions, monoclonal mouse anti-proliferating cell nuclear antigen (PCNA; 1:50; Santa Cruz Biotechnology; Santa Cruz, CA, USA), monoclonal rabbit anti-Ki67 (1:2000; Epitomics; Burlingame, CA, USA), and monoclonal rabbit anti-Caspase-3 (1:25; Epitomics) antibodies were used (Yamada et al., 2011; Guo et al., 2012; Tasaki et al., 2013; Noguchi et al., 2014).

The numbers of positive cells were counted in 10 randomly selected fields in each section (original magnification: 400×) as described previously (Yamada et al., 2011; Guo et al., 2012; Tasaki et al., 2013). All slides were evaluated by two or three independent observers who were blinded to the physical outcome. The agreement between observers was measured to be excellent (>0.9) by the interclass correlation coefficient for all sections investigated.

Terminal deoxynucleotidyl transferase dUTP nick-end labeling (TUNEL) staining

TUNEL assays were performed to detect the death of SMCs *in vivo* using *In Situ* Cell Death Detection Kit PODs (Roche Applied Science; Mannheim, Germany) (Yamada et al., 2011; Guo et al., 2012; Tasaki et al., 2013; Noguchi et al., 2014). The cuffed arteries were labeled with TUNEL reaction mixture (*green*) and anti-human smooth muscle actin antibody, then visualized with goat anti-mouse IgG antibodies conjugated with Alexa Fluor Dyes (*red*) (Invitrogen Corp.) by confocal laser scanning microscopy (LSM5 Pascal Exciter; Carl Zeiss; Oberkochen, Germany; original magnification: 400×) (Tasaki et al., 2013).

Enzyme-linked immunosorbent assay (ELISA) for TNF-α

Serum TNF-α levels were measured at day 10 after cuff injury using an ELISA kit (R&D Systems; Minneapolis, MN, USA) according to the manufacturer's instructions (Noguchi et al., 2014).

Migration assay

Aortic SMCs were isolated from the thoracic aortas of four- to six-week-old male WT and *ATGL*$^{-/-}$ mice by the explant method (Lin et al., 2013). The cultured SMCs (5×10^4 cells, 1 mL) derived from WT and *ATGL*$^{-/-}$ mice were added to the top chamber of a 24-well plate transwell insert (6.5 mm diameter, 3 μm pore size; Becton Dickinson Labware) according to previously reported methods and the manufacturer's instructions (Izumi et al., 2011). Platelet-derived growth factor (PDGF)-BB (10 ng/mL; Peprotech; London, UK) in DMEM (Dulbecco's Modified Eagle Medium) plus 10% FBS (Fetal Bovine Serum) was added to the upper well, whereas TNF-α (100 ng/mL; Sigma; St. Louis, MO, USA) as a chemoattractant was used in the lower well. The chambers were incubated for 22 h at 37°C under an atmosphere of 5% CO_2. The cells on the lower surface of the filters were fixed in 95% acetone and incubated with Hoechst 33258 (0.5 μg/mL; Dojindo; Kumamoto, Japan) after the cells on the upper surface of the filters were removed. The cells were then observed and photographed immediately with an inverted fluorescence microscope (ECLIPSE E600; Nikon, Tokyo, Japan). Ten representative fields (~100 cells) were counted in each experiment and the experiments were repeated more than 10 times. More than 10 experiments were performed independently.

Statistical analysis

All values are expressed as the mean ± standard error. Significant differences were analyzed using Student's t-tests, Welch's t-tests, or one-way analysis of variance (ANOVA), where appropriate. In all cases when ANOVA was employed for non-parametric data, Tukey's multiple comparison post-hoc test was used. Values with P<0.05 were considered statistically significant.

Results

Histological characteristics of cuff-induced vascular remodeling in ATGL$^{-/-}$ mice

Neointimal formation

As shown in Figs. 1, 2, quantitative analysis of the sequential sections from femoral arteries showed that

ATGL$^{-/-}$ mice had significantly accelerated neointimal lesions compared with WT mice after cuff injury-induced vascular remodeling for 10 days (5.14±0.92×10^3 vs. 2.24±0.64×10^3 μm^2, P<0.001) (Figs. 1A, 2A). However, the medial thickness was not significantly different between the *ATGL$^{-/-}$* and WT mice (26.8±0.7 vs. 26.1±1.1 μm, P=0.30) (Fig. 2B). Correspondingly, the intima-to-media ratios (I/M ratios) in *ATGL$^{-/-}$* mice were markedly higher than those in WT mice (0.49±0.04
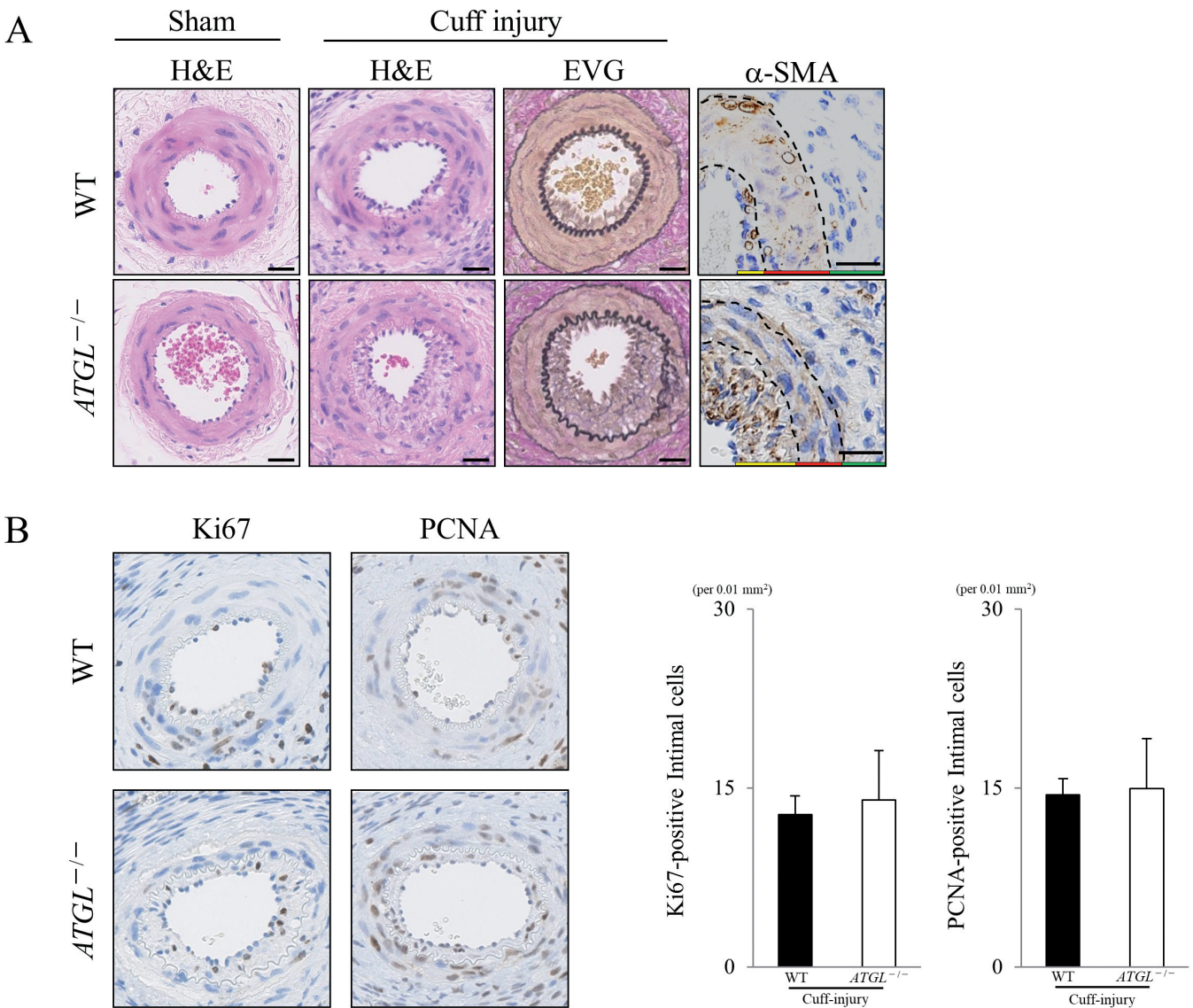

Fig. 1. Histological and immunohistochemistry (IHC) analyses in the intima of cuff-injured femoral arteries and proliferation in the mouse arteries with cuff injury-induced vascular remodeling. **A.** Representative sequential sections of the right femoral arteries in wild-type (WT) and *ATGL*-knockout (*ATGL$^{-/-}$*) mice 10 days after cuff injury. Left femoral arteries without cuff (sham-operated) served as controls. Elastica van Gieson (EVG) staining revealed both internal and external elastic lamina (IEL and EEL). IHC showed that the number of intimal migrated α-SMA+ smooth muscle cells (SMCs) was significantly higher in the neointimal lesions of *ATGL$^{-/-}$* mice than in those of WT mice. Yellow, red, and green lines indicate the intima, media, and adventitia, respectively. **B.** Representative IHC sequential sections of *ATGL$^{-/-}$* mice compared with WT mice which were stained for Ki67 and PCNA. The number of Ki67+ or PCNA+ cells in the thickened neointimal lesions revealed no significant differences between the two groups of mice. The values are the means ± SE. n=8 to 10 mice in each group. Scale bars: 25 μm.

vs. 0.22±0.01, P<0.0001) (Fig. 2C). However, the EEL length was not significantly different between the two groups (514.0±16.5 vs. 515.1±31.9 μm). The stenotic lumen area, the thickened adventitial area, and the total vessel area were not significantly different in the two groups (lumen area: 3.46±0.72×10^3 vs. 4.63±1.19×10^3 μm^2; adventitial area: 89.2±1.0×10^3 vs. 89.1±8.8×10^3 μm^2; total vessel area: 103±10×10^3 vs. 106±9×10^3 μm^2) (Fig. 2D-F). Very few intimal areas and low I/M ratios (intima: 1.24±0.08×10^3 vs. 1.44±0.01×10^3 μm^2; medial thickness: 22.4±0.69 vs. 22.7±1.0 μm; Fig. 2A,B) were observed in sham-operated arteries of the two groups, and there was no significant difference in EEL length

between the two groups (503±21 vs. 504±10 μm). Additionally, there were no significant differences in lumen area, adventitial area, or the total vessel area in sham-operated arteries of the two groups (lumen area: 6.92±1.24×10^3 vs. 6.17±0.79×10^3 μm^2; adventitial area: 11.2±0.5×10^3 vs. 10.3±0.6×10^3 μm^2; total vessel area: 21.0±0.7×10^3 vs. 22.6±0.9×10^3 μm^2) (Fig. 2D-F). Therefore, the present study suggested that the cuff induced concentric-type stenosis. More α-SMA+ SMCs were observed in the neointimal lesions of *ATGL*$^{-/-}$ mice than in WT mice (21.1±2.8 vs. 13.0±3.0/0.01 mm^2; P<0.05) 10 days after cuff injury (Fig. 1A). However, there was no significant difference in the number of
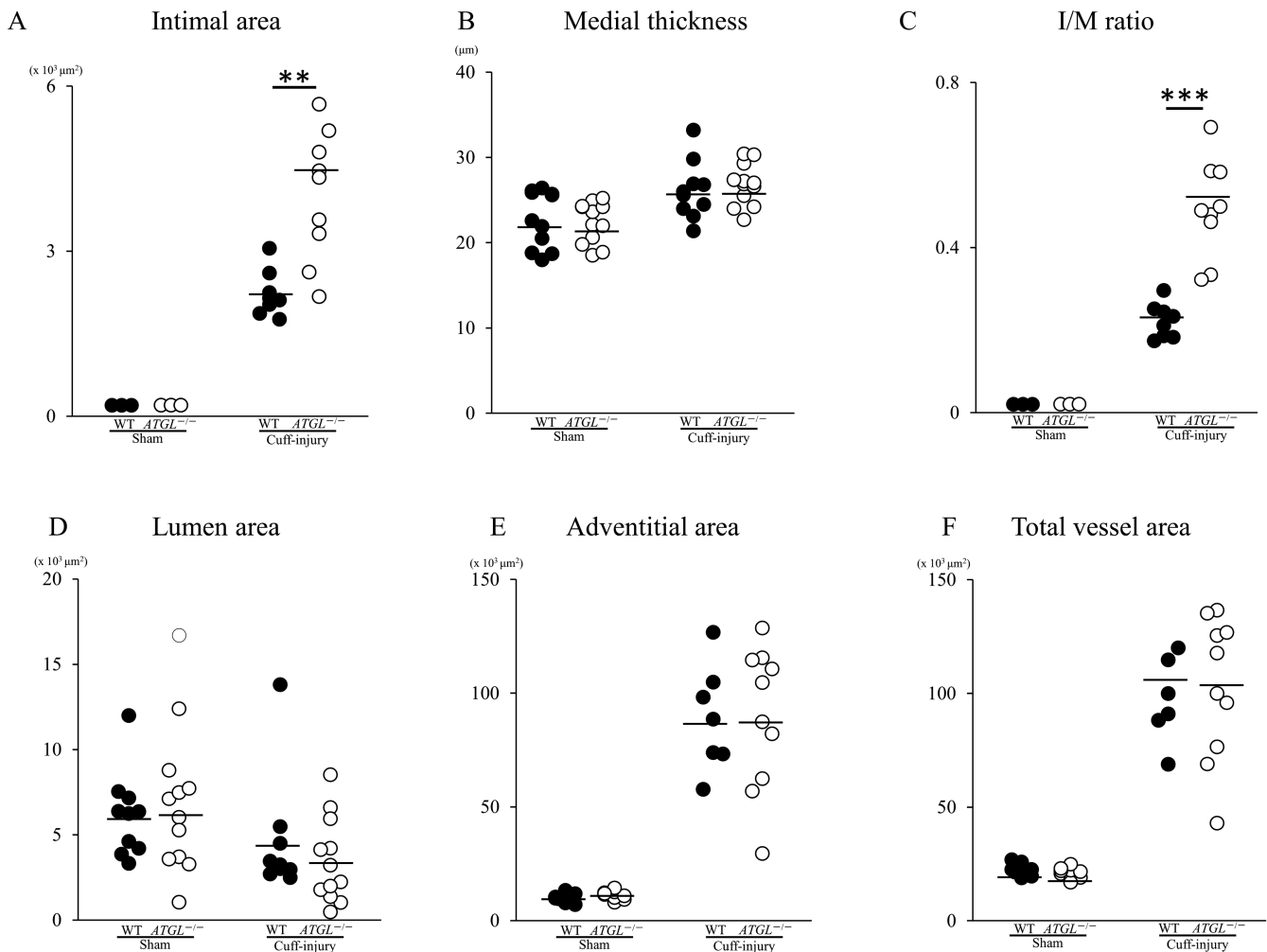

Fig. 2. Histological analyses of intimal area, medial thickness, I/M ratio, lumen area, adventitial area, and total vessel area of cuff-injured femoral arteries. **A.** The quantitative analysis demonstrated that *ATGL*-knockout (*ATGL*$^{-/-}$) mice had significantly accelerated neointimal lesions compared to wild-type (WT) mice in cuff injury-induced vascular remodeling. **B, C.** The *ATGL*$^{-/-}$ mouse arteries with cuff injury-induced vascular remodeling significantly accelerated neointimal lesions compared with the WT mice, but not thickened medial lesions. Thus, the I/M ratio of *ATGL*$^{-/-}$ mice was more markedly increased than that of WT mice. **D-F.** The lumen area, adventitial area, and total vessel area were not significantly (N.S.) different between the two groups of mice. Control arteries from both mice show large lumen areas and a thin medial thickness, along with small adventitial areas and total vessel areas compared to the cuff-placed arteries. All values are shown as mean ± SE. *P<0.05, **P<0.001, ***P<0.0001. n=8 to 12 mice in each group.

medial SMCs between the two groups (13.5±0.8 vs. 13.6±1.2/0.01 mm^2, P=0.48).

As shown in Fig. 1B, there were no significant differences in the percentage of Ki67$^+$ or PCNA$^+$ in the thickened neointimal or medial lesions between *ATGL*$^{-/-}$ and WT mice suggesting that proliferation activities did not change in *ATGL*$^{-/-}$ mice.

Medial cell death and loss of elastic fibers

A substantial amount of cell death was observed in the medial but not in the neointimal SMCs in both groups of mice (Fig. 3A). The number of TUNEL$^+$ medial cells (7.3±1.0 vs. 2.3±0.4/0.01 mm^2, P<0.001) and Caspase-3$^+$ medial cells was significantly higher in the *ATGL*$^{-/-}$ mice than in the WT mice (Fig. 3B). Masson's trichrome and EVG staining revealed larger amounts of cystic mediolysis and elastic fiber loss (Fig. 3C), related to the acellular areas in the medial vascular walls in the *ATGL*$^{-/-}$ mice than in the WT mice. However, Alcian blue staining was negative in these acellular medial lesions (data not shown).
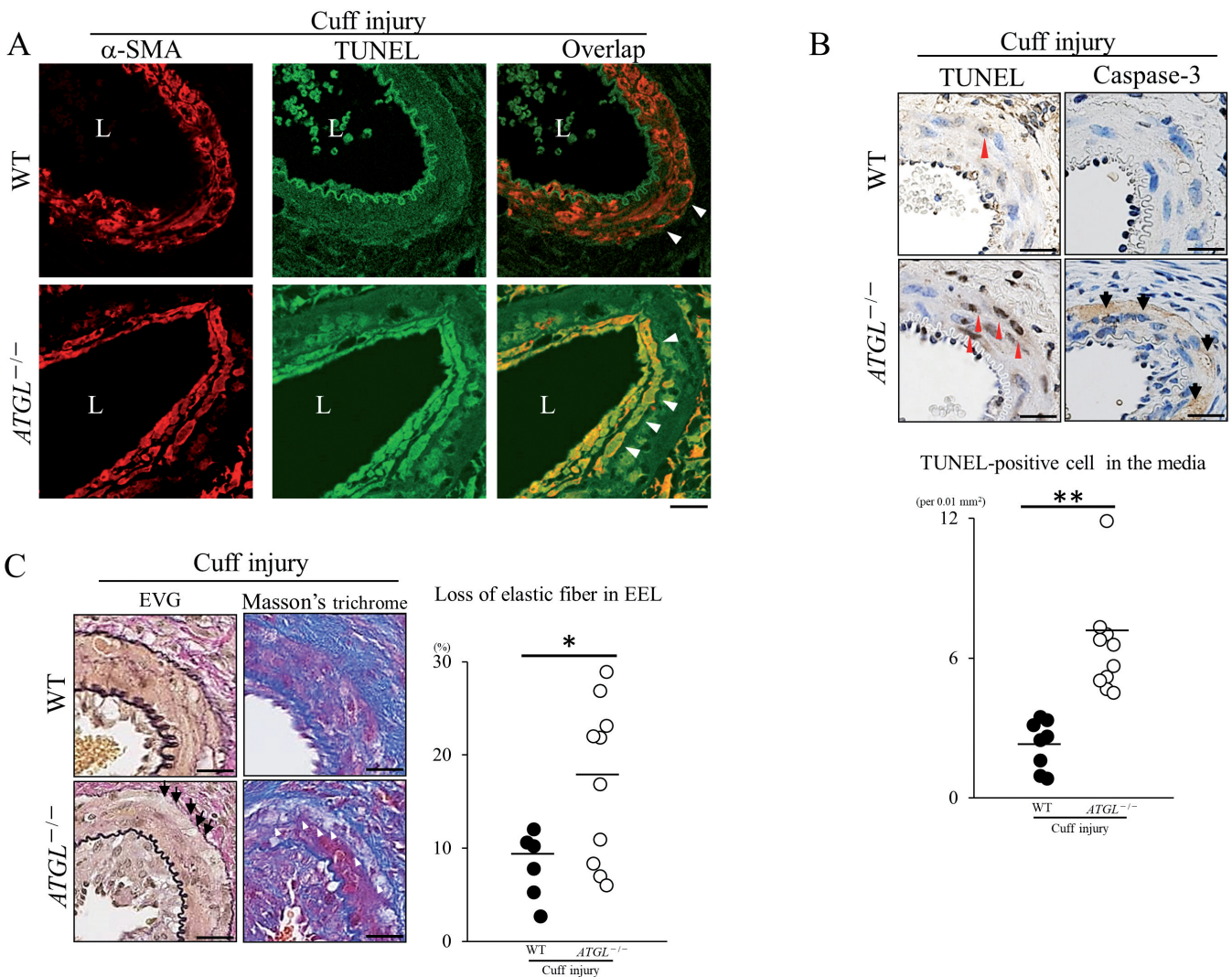

Fig. 3. Terminal deoxynucleotidyl transferase end-labeling (TUNEL) analysis and Elastica van Gieson (EVG) staining of cuff injury-induced vascular remodeling in mouse femoral arteries. **A.** Double-immunofluorescence staining revealed that apoptotic cells (TUNEL+, green) in the media were smooth muscle cells (SMCs) (α-SMA+, red). L: lumen. **B.** The number of TUNEL+ medial cells (arrowheads) were significantly higher in *ATGL*-knockout (*ATGL*$^{-/-}$) mice than in wild-type (WT) mice. Correspondingly, the number of Caspase-3+ medial cells (arrows) were significantly higher in *ATGL*$^{-/-}$ mice than in WT mice. **C.** Representative sequential sections revealed significantly greater loss of medial elastic fibers (arrows) and larger amounts of cystic mediolysis (arrowheads) by EVG and Masson's trichrome staining, respectively. This most likely corresponded to the acellular areas in the medial vascular walls in the cuff-injured arteries of *ATGL*$^{-/-}$ mice, compared with those of WT mice. All values are shown as mean ± SE. *P<0.05, **P<0.001, ***P<0.0001. n=8 to 10 mice in each group. Scale bars: 25 *μ*m.

Infiltrating cells with expression of TNF-α in the tunica adventitia

The number of adventitial Mac-2^{+} cells was significantly higher in the *ATGL*^{−/−} mice than in the WT mice (10.5±0.6 vs. 8.0±0.6, P<0.05) (Fig. 4A). However, the number of Gr-1^{+} neutrophils in the adventitia was not significantly different between the two groups (data not shown). The numbers of neointimal Mac-2^{+} cells in each cross-section were very low in both the *ATGL*^{−/−}

and WT mice (1.5±0.5 vs. 2.2±0.8/0.01 mm^2, P=0.21). The IF study showed that the number of TNF-α^{+} adventitial cells was greater in the injured arteries of *ATGL*^{−/−} mice than in WT mice (6.8±0.7 vs. 4.8±0.9, P<0.05). The number of TNF-α[+] and Mac-2^{+} cells in the tunica adventitia was also significantly higher in the *ATGL*^{−/−} mice than in the WT mice 10 days after cuff injury (Fig. 4B). Similarly, the ELISA results demonstrated that serum TNF-α levels were markedly higher in *ATGL*^{−/−} mice than in WT mice (12.39±0.99
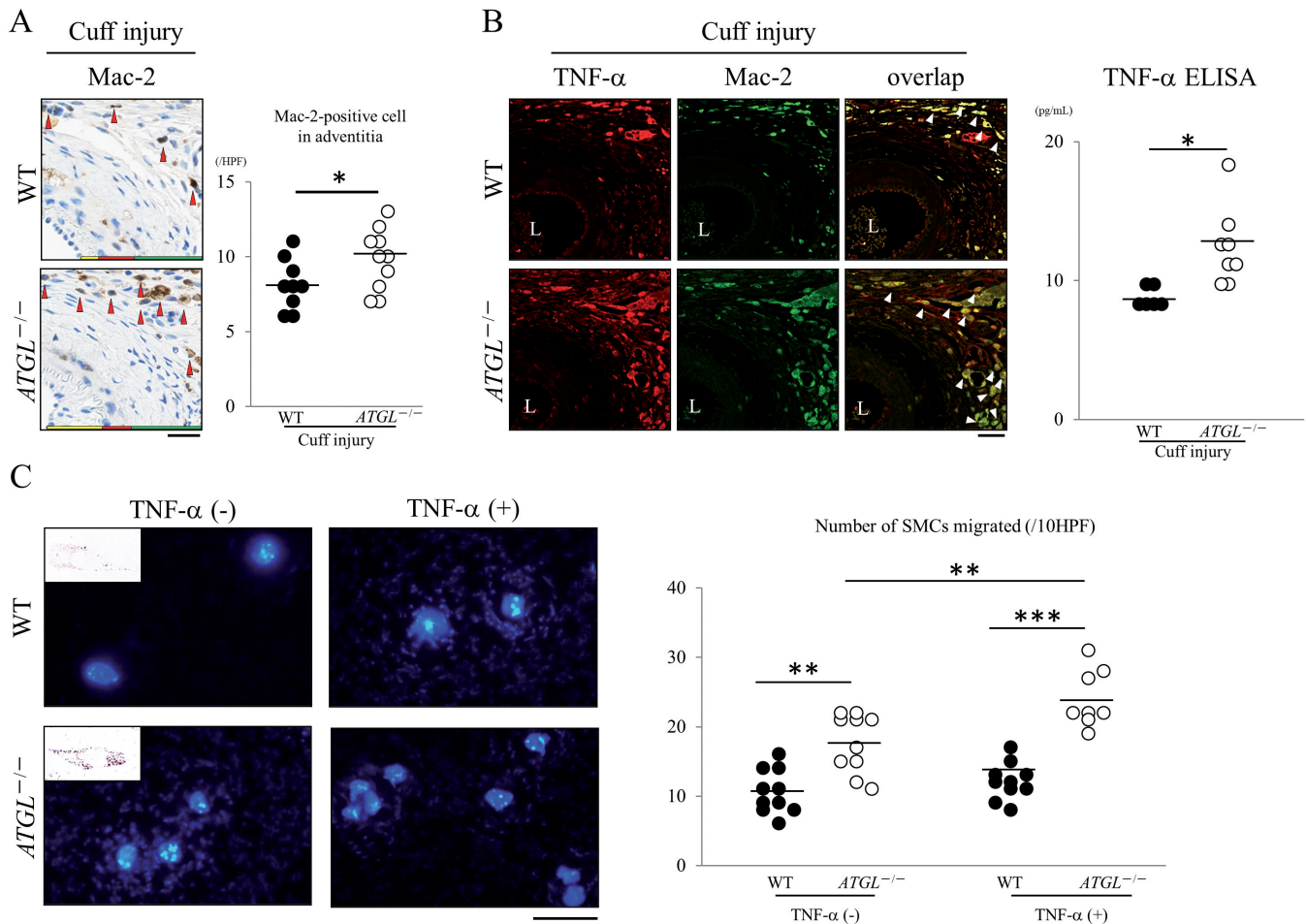

Fig. 4. Perivascular reactions in the mouse arteries with cuff injury-induced vascular remodeling and migration of wild-type (WT) and *ATGL*-knockout (*ATGL*^{−/−}) mouse aortic smooth muscle cells (SMCs). **A.** IHC revealed that the number of adventitial Mac-2+ cells was significantly higher in the inflamed perivascular lesions of *ATGL*^{−/−} mice (arrowheads) than in those of WT mice. In contrast, the numbers of neointimal and medial inflammatory cells was not significantly different between the two groups of mice. Yellow, red, and green lines indicate the intima, media, and adventitia, respectively. **B.** The immunofluorescence (IF) study showed that the number of tumor necrosis factor-α+ (TNF-α+) perivascular cells (red-stained) was higher in the injured arteries of *ATGL*^{−/−} mice than in WT mice. Additionally, the number of TNF-α+ (red-stained) and Mac-2+ (green-stained) double positive perivascular infiltrating cells was significantly higher in the *ATGL*^{−/−} mice than in the WT mice (arrowheads). Correspondingly, the enzyme-linked immunosorbent assay (ELISA) results demonstrated that serum TNF-α levels were significantly higher in *ATGL*^{−/−} mice than in WT mice. L: lumen. The values are shown as mean ± SE. n=8 to 10 mice in each group. **C.** Representative photographs showing overt lipid accumulated (red-stained) aortic SMCs with spindled structures in *ATGL*^{−/−} mice, but absent or weak accumulation in WT mice (insets) by optimized oil red-O staining. Migration assays showed that platelet-derived growth factor (PDGF)-BB (10 ng/mL in top chamber) as well as TNF-α (100 ng/mL in bottom chamber) had a chemotactic effect on the cultured aortic SMCs. The number of PDGF-BB-induced migrated SMCs was significantly higher in the *ATGL*^{−/−} mice than in the WT mice 22 h after incubation, with an additive effect of TNF-α. Values are shown as mean ± SE of at least 10 separate experiments (n=10 per condition). *P<0.05, **P<0.001, ***P<0.0001. Scale bars: 25 *μ*m.

vs. 8.76±0.30 pg/mL, P<0.05; Fig. 4B), whereas TNFα levels were markedly low in both uninjured $ATGL^{-/-}$ and WT mice (0.31±0.10 and 0.0±0.0 pg/mL, respectively), compared with cuff-injured mice.

In vitro migration assay (Boyden chamber) of ATGL-deficient SMCs

Oil red-O staining indicated more lipid accumulation in SMCs (*red stain*) with spindle structures in $ATGL^{-/-}$ mice than in WT mice (left panel inset, Fig. 4C). In the migration assay, PDGF-BB had a chemotactic effect on cultured aortic SMCs, and the number of migrated SMCs was significantly higher in the $ATGL^{-/-}$ mice than in the WT mice (17.7±1.3 vs. 10.6±1.0, P<0.001). A combination of TNF-α and PDGF-BB resulted in a higher number of migrated SMCs in the $ATGL^{-/-}$ mice than in the WT mice (24.0±1.5 vs. 12.1±0.8, P<0.0001) and $ATGL^{-/-}$ mice with PDGF-BB stimulation alone (Fig. 4C).

Discussion

In the present study, for the first time, we demonstrated the effect of cuff injury on the femoral arteries of $ATGL^{-/-}$ mice. Table 1 summarizes the experimental results in $ATGL^{-/-}$ mice 10 days after cuff injury. The $ATGL^{-/-}$ mice had potentially pro-atherogenic profiles with phenotypes of SMCs that mimic atherosclerotic lesions in patients with TGCV (Hirano, et al., 2008, Ikeda, et al., 2014b, Li, et al., 2019). The SMCs showed two distinct phenotypes: (i) significant migratory activities compared to the SMCs in injured WT mice, but proliferative activities comparable to SMCs in $ATGL^{-/-}$ and WT mice; and (ii) accelerated medial cell death. The induction of medial SMC death can cause elastolysis and degeneration, and is associated with changes in the composition of the extracellular matrix and subsequent failure of outward (i.e., expansive) vessel remodeling (Clarke et al., 2008). Adventitial infiltration of Mac-2⁺ cells expressing TNF-α increased, and migration of SMCs responding to TNF-α was higher in $ATGL^{-/-}$ than in WT mice.

It would be of interest to know the details of the mechanism underlying the vascular changes observed in cuff-injured $ATGL^{-/-}$ mice. As far as we know, our study is the first to investigate serum levels of TNF-α in cuff-injured models. In both $ATGL^{-/-}$ and WT mice, TNF-α levels were much higher than those of uninjured mice, which suggested that adventitial cells expressing TNF-α may be a major source for high levels of serum TNF-α. In addition, we observed that TNF-α levels in serum were significantly higher in cuff-injured $ATGL^{-/-}$ than in cuff-injured WT mice. Although the details of the mechanism underlying the additional increase in $ATGL^{-/-}$ mice is unknown, the overexpression of TNF-α has been reported in other cellular models with ATGL deficiency (Schrammel et al., 2013). We think that TNF-α may be one of the major contributors for the outside-in signaling in cuff-injured $ATGL^{-/-}$ mice. Kitagaki et al. (2012) previously reported that inhibition of TNF-α signaling by the intraperitoneal administration of TNF-α receptor 1 antagonist ameliorated vascular changes in cuff-injured mice with a deficiency of interleukin-1 receptor antagonist.

As described above, the vascular changes observed in the femoral arteries of cuff-injured $ATGL^{-/-}$ mice pathologically mimic the findings in coronary arteries of patients with TGCV. However, our study has the following limitations when the experimental results are extrapolated to human diseases, because $ATGL^{-/-}$ mice die around at the age of 13-15 weeks due to heart failure with cardiomyocyte steatosis (Haemmerle et al., 2006). Atherosclerosis is a chronic and complex process consisting of initiation, progression, and regression of lesions. This model may be suitable for the investigation of the progression process and its underlying mechanism, but not for the regression process with pharmaceutical intervention.

In conclusion, outside-in signaling by cuff injury induced a distinct vascular lesion with exacerbation of perivascular expression of TNF-α in Mac-2⁺ cells, mediolysis, and neointimal formation of SMCs in $ATGL^{-/-}$ mice. Cuff injury might be a model to understand the mechanisms underlying the development of atherosclerotic lesions observed in patients with TGCV, although further studies are required to investigate the molecular mechanisms underlying the enhanced cellular responses to cuff injury in ATGL deficiency.

Table 1. Summary of experiments.

	$ATGL^{-/-}$ mice, compared with WT
Cuff injury experiment (*in vivo*)	
Neointimal formation	↑
Proliferation markers* in intimal SMCs	→
Cell death markers** in medial SMCs	↑
Loss of elastic fiber in media	↑
Perivascular TNF-α expression	↑
Boyden chamber experiment (*in vitro*)	
Migrating activity of SMCs in response to TNF-α***	↑

*Ki67, PCNA. **TUNEL, Caspase-3. ***Under condition with PDGF BB.

References

Booth R.F., Martin JF, Honey A.C., Hassall D.G., Beesley J.E. and Moncada S. (1989). Rapid development of atherosclerotic lesions in the rabbit carotid artery induced by perivascular manipulation. Atherosclerosis 76, 257-268.

Clarke M.C., Littlewood T.D., Figg N., Maguire J.J., Davenport A.P., Goddard M. and Bennett M.R. (2008). Chronic apoptosis of vascular smooth muscle cells accelerates atherosclerosis and promotes calcification and medial degeneration. Circ. Res. 102, 1529-1538.

Daugherty A., Tall A.R., Daemen M.J.A.P., Falk E., Fisher E.A., García-Cardeña G., Lusis A.J., Owens A.P. 3rd., Rosenfeld M.E. and Virmani R. (2017). Recommendation on design, execution, and reporting of animal atherosclerosis studies. A scientific statement from the American Heart Association. Arterioscler. Thromb. Vasc. Biol. 37, e131-e157.

Fazio S. and Linton M.F. (1996). Murine bone marrow transplantation as a novel approach to studying the role of macrophages in lipoprotein metabolism and atherogenesis. Trends Cardiovasc. Med. 6, 58-65.

Guo X., Yamada S., Tanimoto A., Ding Y., Wang K.Y., Shimajiri S., Murata Y., Kimura S., Tasaki T., Nabeshima A., Watanabe T., Kohno K. and Sasaguri Y. (2012). Overexpression of peroxiredoxin 4 attenuates atherosclerosis in apolipoprotein E knockout mice. Antioxid. Redox. Signal. 17, 1362-1375.

Haemmerle G., Lass A., Zimmermann R., Gorkiewicz G., Meyer C., Rozman J., Heldmaier G., Maier R., Theussl C., Eder S., Kratky D., Wagner E.F., Klingenspor M., Hoefler G. and Zechner R. (2006). Defective lipolysis and altered energy metabolism in mice lacking adipose triglyceride lipase. Science 312, 734-737.

Hirano K. (2009). A novel clinical entity: triglyceride deposit cardiomyovasculopathy. J. Atheroscler. Thromb. 16, 702-705.

Hirano K., Ikeda Y., Zaima N., Sakata Y. and Matsumiya G. (2008). Triglyceride deposit cardiomyovasculopathy. N. Engl. J. Med. 359, 2396-2398.

Hirano K., Tanaka T., Ikeda Y., Yamaguchi S., Zaima N., Kobayashi K., Suzuki A., Sakata Y., Sakata Y., Kobayashi K., Toda T., Fukushima N., Ishibashi-Ueda H., Tavian D., Nagasaka H., Hui S.P., Chiba H., Sawa Y. and Hori M. (2014). Genetic mutations in adipose triglyceride lipase and myocardial up-regulation of peroxisome proliferated activated receptor-g in patients with triglyceride deposit cardiomyovasculopathy. Biochem. Biophys. Res. Commun. 443, 574-579.

Hirano K., Li M. and Ikeda Y. (2019). Triglyceride deposit cardiomyovasculopathy. In: Human pathobiochemistry: from clinical studies to molecular mechanisms. Oohashi T., Tsukahara H., Ramirez F., Barber C.L. and Otsuka F. (eds.). Springer. Singapore. pp 111-119.

Ikeda Y., Hirano K., Fukushima N. and Sawa Y. (2014a). A novel type of human spontaneous coronary atherosclerosis with triglyceride deposition. Eur. Heart J. 35, 875.

Ikeda Y., Zaima N., Hirano KI., Mano M., Kobayashi K., Yamada S., Yamaguchi S., Suzuki A., Hamasaki T., Kotani J., Kato S., Ngasaki H., Setou M. and Ishibasi-Ueda H. (2014b). Coronary triglyceride deposition in contemporary advanced diabetics. Pathol. Int. 64, 325-335.

Izumi H., Takahashi M., Uramoto H., Nakayama Y., Oyama T., Wang K.Y., Sasaguri Y., Nishizawa S. and Kohno K. (2011). Monocarboxylate transporters 1 and 4 are involved in the invasion activity of human lung cancer cells. Cancer Sci. 102, 1007-1013.

Kitagaki M., Isoda K., Kamada H., Kobayashi T., Tsunoda S., Tsutsumi Y., Niida T., Kujiraoka T., Ishigami N., Ishihara M., Matsubara O., Ohsuzu F. and Kikuchi M. (2012) Novel TNF-α receptor 1 antagonist treatment attenuates arterial inflammation and intimal hyperplasia in mice. J. Atheroscler. Thromb. 19, 36-46.

Kockx M.M., De Meyer G.R., Jacob W.A., Bult H. and Herman A.G. (1992). Triphasic sequence of neointimal formation in the cuffed carotid artery of the rabbit. Arterioscler. Thromb. 12, 1447-1457.

Kozawa J., Higashi M., Shimomura I. and Hirano K. (2019). Intractablec coronary artery disease in a type 2 diabetic patient presenting with triglyceride deposit cardiomyovasculopathy. Diabetes Care 42, 983-986.

Lammers B., Chandak P.G., Aflaki E., van Puijvelde G.H., Radovic B., Hildebrand R.B., Meurs I., Out R., Kuiper J., van Berke T.J., Kolb L.D., Haemmerle G., Zechner R., van Eck S., Levak-Frank M. and Kratky D. (2011). Macrophage adipose triglyceride lipase deficiency attenuates atherosclerotic lesion development in low-density lipoprotein receptor knockout mice. Arterioscler. Thromb. Vasc. Biol. 31, 67-73.

Li M., Hirano K., Ikeda Y., Higashi M., Hashimoto C., Zhang B., Kozawa J., Sugimura K., Miyauchi H., Suzuki A., Hara Y., Takagi A., Ikeda Y., Kobayashi K., Futsukaichi Y., Zaima N., Yamaguchi S., Shrestha R., Nakamura H., Kawaguchi K., Sai E., Hui S.P., Nakano Y., Sawamura A., Inaba T., Sakata Y., Yasui Y., Nagasawa Y., Kinugawa S., Shimada K., Yamada S., Hao H., Nakatani D., Ide T., Amano T., Naito H., Nagasaka H. and Kobayashi K. (2019). Triglyceride deposit cardiomyovasculopathy: A rare cardiovascular disorder. Orphanet. J. Rare Dis. 14, 134.

Lin Y., Chiba S., Suzuki A., Yamaguchi S., Nakanishi T., Matsumoto H., Ikeda Y., Ishibashi-Ueda H., Hirano K. and Kato S. (2013). Vascular smooth muscle cells isolated from adipose triglyceride lipase-deficient mice exhibit distinct phenotype and phenotypic plasticity. Biochem. Biophys. Res. Commun. 434, 534-540.

Moroi M., Zhang L., Yasuda T., Virmani R., Gold H.K., Fishman M.C. and Huang P.L. (1998). Interaction of genetic deficiency of endothelial nitric oxide, gender, and pregnancy in vascular response to injury in mice. J. Clin. Invest. 101, 1225-1232.

Nakajima K. (2021). Triglyceride deposit cardiomyovasculopathy: how to recognise a new disease entity. Heart 107, 93-95.

Nakano Y., Suzuki M., Hirano K., Ando H., Takashima H., Takahashi H. and Amano T. (2020). Association of triglyceride deposit cardiomyovasculopathy with drug-eluting stent restenosis among patients with diabetes. JAMA Netw. Open 3, e2012583.

Noguchi H., Yamada S., Nabeshima A., Guo X., Tanimoto A., Wang K.Y., Kitada S., Tasaki T., Takama T., Shimajiri S., Horlad H., Komohara Y., Izumi H., Kohno K., Ichijo H. and Sasaguri Y. (2014). Depletion of apoptosis signal-regulating kinase 1 prevents bile duct ligation-induced necroinflammation and subsequent peribiliary fibrosis. Am. J. Pathol. 184, 644-661.

Onishi T., Nakano Y., Hirano K., Nagasawa Y., Niwa T., Tajima A., Ishii H., Takahashi H., Sakurai S., Ando H., Takashima H. and Amano T. (2021). Prevalence and clinical outcomes of triglyceride deposit cardiomyovasculopathy among hemodialysis patients. Heart 107, 127-134.

Ross R. and Glomset J.A. (1973). Atherosclerosis and the arterial smooth muscle cell: proliferation of smooth muscle is a key event in the genesis of the lesions of atherosclerosis. Science 180, 1332-1339.

Ross R. (1999). Atherosclerosis--an inflammatory disease. N. Engl. J.

Med. 340, 115-126.

Sasaguri Y., Wang K.Y., Tanimoto A., Tsutsui M., Ueno H., Murata Y., Kohno Y., Yamada S. and Ohtsu H. (2005). Role of histamine produced by bone marrow-derived vascular cells in pathogenesis of atherosclerosis. Circ. Res. 96, 974-981.

Schrammel A., Mussbacher M., Winkler S., Haemmerle G., Stessel H., Wölkart G., Zechner R. and Mayer B. (2013) Cardiac oxidative stress in a mouse model of neutral lipid storage disease. Biochem. Biophys. Acta 1831, 1600-1608.

Tasaki T., Yamada S., Guo X., Tanimoto A., Wang K.Y., Nabeshima A., Kitada S., Noguchi H., Kimura S., Shimajiri S., Kohno K., Ichijo H. and Sasaguri Y. (2013). Apoptosis signal-regulating kinase 1 deficiency attenuates vascular injury-induced neointimal hyperplasia by suppressing apoptosis in smooth muscle cells. Am. J. Pathol. 182, 597-609.

Yamada S., Wang K.Y., Tanimoto A., Fan J., Shimajiri S., Kitajima S., Morimoto M., Tsutsui M., Watanabe T., Yasumoto K. and Sasaguri Y. (2008). Matrix metalloproteinase 12 accelerates the initiation of atherosclerosis and stimulates the progression of fatty streaks to fibrous plaques in transgenic rabbits. Am. J. Pathol. 172, 1419-1429.

Yamada S., Ding Y., Tanimoto A., Wang K.Y., Guo X., Li Z., Tasaki T., Nabesima A., Murata Y., Shimajiri S., Kohno K., Ichijo H. and Sasaguri Y. (2011). Apoptosis signal-regulating kinase 1 deficiency accelerates hyperlipidemia-induced atheromatous plaques via suppression of macrophage apoptosis. Arterioscler. Thromb. Vasc. Biol. 31, 1555-1564.

Yamada S., Wang K.Y., Tanimoto A., Guo X., Nabeshima A., Watanabe T. and Sasaguri Y. (2013). Histamine receptors expressed in circulating progenitor cells have reciprocal actions in ligation-induced arteriosclerosis. Pathol. Int. 63, 435-447.

Yamada S., Tanimoto A. and Sasaguri Y. (2016). Critical *in vivo* roles of histamine and histamine receptor signaling in animal models of metabolic syndrome. Pathol. Int. 66, 661-671.

Zechner R., Kienesberger P.C., Haemmerle G., Zimmermann R. and Lass A. (2009). Adipose triglyceride lipase and the lipolytic catabolism of cellular fat stores. J. Lipid Res. 50, 3-21.

Zimmermann R., Strauss J.G., Haemmerle G., Schoiswohl G., Birner-Gruenberger R., Riederer M., Lass A., Neuberger G., Eisenhaber F., Hermetter A. and Zechner R. (2004). Fat mobilization in adipose tissue is promoted by adipose triglyceride lipase. Science 306, 1383-1386.